Journal of Macromolecular Science, Part A: Pure and Applied Chemistry (2011) **48**, 713–721

ISSN: 1060-1325 print / 1520-5738 online
DOI: 10.1080/10601325.2011.596050

Taylor & Francis
Taylor & Francis Group

Preparation, Characterization and Optimization of Chitosan Nanoparticles as Carrier for Immobilization of Thermophilic Recombinant Esterase

HÜSEYIN İLGÜ, TAYLAN TURAN, and GÜLŞAH ŞANLI-MOHAMED*

İzmir Institute of Technology, Science Faculty, Department of Chemistry, Urla, İzmir, Turkey

Received February 2011, Accepted March 2011

Immobilization of biologically important molecules on myriad nano-sized materials has attracted great attention. Through this study, thermophilic esterase enzyme was obtained using recombinant DNA technology and purified applying one-step His-Select HF nickel affinity gel. The synthesis of chitosan was achieved from chitin by deacetylation process and degree of deacetylation was calculated as 89% by elemental analysis. Chitosan nanoparticles were prepared based on the ionic gelation of chitosan with tripolyphosphate anions. The physicochemical properties of the chitosan and chitosan nanoparticles were determined by several methods including SEM (Scanning Electron Microscopy), FT-IR (Fourier Transform Infrared Spectroscopy) and DLS (Dynamic Light Scattering). The morphology of chitosan nanoparticles was spherical and the nanospheres' average diameter was 75.3 nm. The purified recombinant esterase was immobilized efficiently by physical adsorption onto chitosan nanoparticles and effects of various immobilization conditions were investigated in details to develope highly cost-effective esterase as a biocatalyst to be utilized in biotechnological purposes. The optimal conditions of immobilization were determined as follows; 1.0 mg/mL of recombinant esterase was immobilized on 1.5 mg chitosan nanoparticles for 30 min at 60°C, pH 7.0 under 100 rpm stirring speed. Under optimized conditions, immobilized recombinant esterase activity yield was 88.5%. The physicochemical characterization of enzyme immobilized chitosan nanoparticles was analyzed by SEM, FT-IR and AFM (Atomic Force Microscopy).

Keywords: Esterase, chitosan, nanoparticle, immobilization

1 Introduction

Enzymes are an important tool in a wide variety of biotechnological applications, but the utilization of them as a free form is not preferable due to their undesirable features. Hence, immobilization of enzymes is crucial for effective utilization and reusability of enzymes in many industrial processes. As compared to free enzymes in solution, immobilized enzymes are more robust and more resistant to environmental changes (1, 2). Therefore, many kinds of immobilization techniques have been improved for many years on various supports via different methods (3–7).

Recently, researchers have indicated that nano-sized materials can be used for immobilization of enzymes due to attractive characteristics of nano-materials such as small size, magnetism and large surface area (8). One of the most used biopolymer as immobilization carriers, chitosan, a poly-N-acetyl glucosamine, is the N-deacetylated product of chitin (major component of crustacean shells) which is the second most abundant biopolymer after cellulose (9). Chitosan has many significant biological and chemical properties due to a unique set of characteristics that include biocompatibility, biodegradability to harmless products, nontoxicity, physiological inertness, antibacterial properties, heavy metal ions chelation, gel forming properties, hydrophilicity and remarkable affinity to proteins (10–12). Although, many studies have been conducted about the preparation of chitosan nanoparticles and their applications as the carrier of drugs (13, 14), studies of enzyme immobilization on chitosan nanoparticles have been rarely reported. According to our knowledge, especially, the effects of immobilization conditions on immobilization efficiency and enzyme loading capacity with chitosan nanoparticles have not been previously examined in details. In the development of highly cost-effective biocatalysts, the enzyme efficiency is greatly affected by enzyme loading onto support materials therefore determination of optimum enzyme loading capacity with respect to the enzyme efficiency is commercial interest.

*Address correspondence to: Gülşah Şanlı-Mohamed, İzmir Institute of Technology, Science Faculty, Department of Chemistry, Urla, İzmir, Turkey. Tel: +90 2327507618; Fax: +90 2327507509. E-mail: gulsahsanli@iyte.edu.tr

Since esterase enzymes are of special interest in a variety of biotechnological, industrial, environmental and pharmaceutical applications because of their many useful properties (15–17), in this study, for the first time, we have used thermophilic recombinant esterase enzyme from Balçova Geothermal region (18) for immobilization on chitosan nanoparticles. After synthesis of chitosan from chitin was successfully achieved and chitosan nanoparticles were well prepared, effects of immobilization conditions in terms of enzyme concentration, chitosan nanoparticle amount, immobilization pH, temperature, time and stirring speed on immobilization efficiency and enzyme loading capacity have been examined in detail for the effective utilization of esterase in a wide variety of processes effectively.

2 Experimental

2.1 Materials

For the purpose of chitosan nanoparticle preparation, chitin and sodium tripolyphosphate pentabasic (TPP) were purchased from Sigma; sodium hydroxide anhydrous and acetic acid glacial were purchased from Carlo Erba. All other reagents and solvents were of analytical grade.

2.2 Synthesis and Characterization of Chitosan

Chitosan was synthesized from chitin by the method of Rigby and Wolfrom with some modification described by Boyacı et al. (19). In the procedure, 15.0 g chitin was treated with 720.0 mL of 40.0% (w/w) aqueous NaOH solution at 115°C for 6 h under inert atmosphere. The chitosan then was washed with distilled water and dried at 60°C for 2 h before use.

Several methods were used for the characterization of chitosan. Functional groups of chitosan were characterized using FT-IR (Perkin-Elmer Spectrum 100). The elemental composition and degree of deacetylation of chitosan were determined by a LECO-CHNS-932 elemental analyzer (Mönchengladbach, Germany) and degree of deacetylation was calculated (20). Molecular weight of chitosan was determined using a viscosimetric method at the room temperature (19). Images of chitin and chitosan were taken with SEM (Philips XL-30S FEG, Eindhoven, The Netherlands).

2.3 Preparation and Characterization of Chitosan Nanoparticles

Chitosan nanoparticles were prepared using the method readily constituted by Jiayin and Jianmin (21) with some modifications. In the procedure, 0.5 g of chitosan was dissolved in 100.0 mL 1.0% (v/v) acetic acid glacial and the pH of solution was adjusted to 4.7 with NaOH. Nanoparticles were spontaneously obtained upon the addition of 1.0 mL of 0.25% (w/v) TPP to the chitosan aqueous solution dropwise by automatic micropipette under magnetic stirring at room temperature. After one hour incubation, the solution was centrifuged at 13,500 rpm for 30 min and chitosan nanoparticles were pelleted as transparent gel. The pellet of chitosan nanoparticles was dried by a freeze dryer before characterization.

Chitosan nanoparticles were characterized with several methods. Their surface morphologies and structures were examined by SEM (Philips XL-30S FEG, Eindhoven, The Netherlands). The size distribution of chitosan nanoparticles was obtained by DLS (Malvern Zetasizer, 3000 HSA). Changes in functional groups of chitosan after being nanoparticle were characterized using FT-IR (Perkin-Elmer Spectrum 100).

2.4 Preparation of Recombinant Esterase Enzyme

E.coli BL21(DE3) harboring the IPTG inducible plasmid pET-28a(+) encoding for thermophilic esterase enzyme was expressed and purified applying one step affinity chromatography according to procudure described by Tekedar and Şanlı-Mohamed (19). Quantitative protein determination was spectrophotometrically measured at 595 nm according to Bradford's method (22). Bovine serum albumin was used as a standard protein.

2.5 Immobilization and Characterization of Recombinant Esterase on Chitosan Nanoparticles

In the immobilization procedure, 1.0 mL of phosphate buffer (50.0 mM and pH 7.0) containing 1.5 mg chitosan nanoparticles were incubated with 1.0 mL of pure recombinat esterase enzyme solution (1.0 mg/mL) for 30 min at 60°C under 100 rpm stirring condition. Immobilized enzyme on chitosan nanoparticles were obtained by centrifiguation at 3000 g for 20 min. The supernatant was collected to calculate the residual amount of recombinant esterase enzyme. The amount of esterase enzyme was determined in clear supernatant by UV spectrophotometry (ShimadzuUV-1601, Shimadzu Co. Ltd., Japan) at 280 nm using supernatant of nonloaded nanoparticles as a basic correction.

Enzyme immobilized chitosan nanoparticles were characterized by AFM, SEM and FT-IR spectroscopy.

2.6 Optimization of Conditions for Esterase Immobilization on Chitosan Nanoparticles

To optimize enzyme immobilization efficiency and enzyme loading capacity of recombinant esterase on chitosan nanoparticles, various immobilization conditions for; optimum pH (5, 6 7, 8, 9 and 11), amount of chitosan nanoparticles (0.5, 0.8, 1.0, 1.5, 2.0, 2.5, 3.0 mg/mL), enzyme concentration (0.25, 0.5, 1.0, 2.0, 3.5 and 8.5 mg/mL),

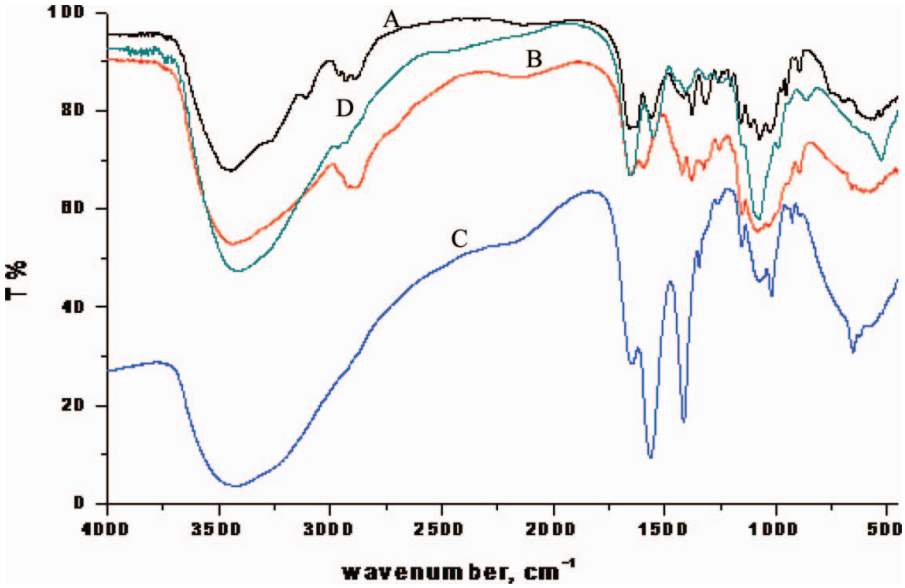

Fig. 1. FT-IR spectra of (A) chitin, (B) chitosan, (C) chitosan nanoparticle, (D) enzyme immobilized chitosan nanoparticles. (Color figure available online.)

immobilization time (5, 30, 60, 120 and 180 min), optimum temperature (15, 25, 37, 50 and 60°C) and immobilization speed (50, 100, 200, 300 and 400 rpm) were screened. Free esterase was determined in the clear supernatant after immobilization using UV spectrophotometry at 280 nm. Esterase immobilization efficiency (IE) and enzyme loading capacity (LC) on chitosan nanoparticles were calculated according to the equations indicated below:

$$\text{IE} = (\text{Total Esterase} - \text{Free Esterase}/\text{Total Esterase}) \times 100 \quad (1)$$

$$\text{LC} = (\text{Total Esterase} - \text{Free Esterase}/\text{Nanoparticles weight}) \times 100 \quad (2)$$

2.7 Activity Measurement of Free and Immobilized Esterase

The free and immobilized esterase activity was assayed according to the procedure described by Tekedar and Şanlı-Mohamed (19) with minor modifications. The assay mixture (1.0 mL) contained 0.5 mM pNPC$_2$ substrate dissolved in acetonitrile including 0.5 mM phosphate buffer at pH 7.0. 0.1 mg/mL purified enzyme or 0.1 mg immobilized enzyme was used and initial rates were estimated by measuring the increase in absorbance at 400 nm as a function of time at 55°C. One unit of esterase activity was defined as the amount of enzyme releasing 1.0 μmol of p-nitrophenol per minute at pH 7.2 at 55°C using pNPC$_2$ as a substrate.

3 Results and Discussion

3.1 Characterization of Chitosan

Chitosan was synthesized from chitin by deacetylation process and degree of deacetylation was calculated as 89% by elemental analysis method. The ratios of C/N were used in the determination of degree of deacetylation by using Equation 3 (23).

$$D.D = \left(1 - \frac{C/N - 5.145}{6.816 - 5.145}\right) \times 100 \quad (3)$$

In the formula, 5.145 is the C/N ratio of completely N-deacetylated chitosan repeating unit and 6.816 is the C/N ratio of N-acetylated chitin repeating unit. The degree of deacetylation of chitosan obtained was in good agreement (89%) with other studies in the literature (19).

FT-IR studies of chitin and chitosan were performed to characterize the functional groups of chitosan by comparing chemical structure of chitin in Figure 1(A) and 1(B). The FT-IR spectra of chitin and chitosan are compatible with the literature studies (24, 25). The absorption bands at 1595 and 1650 cm^{-1} in chitosan were referenced to the N-H bending in primary amine and amide I bands, respectively.

3.2 Characterization of Chitosan Nanoparticles

The preparation of the chitosan nanoparticles was based on ionic gelation interactions between the positively charged polymer and negatively charged TPP. Since the complexation process is very simple and mild, chitosan nanoparticles has recently attracted much attention (19). The size distribution of chitosan nanoparticles were characterized by dynamic light scattering measurements attributed to

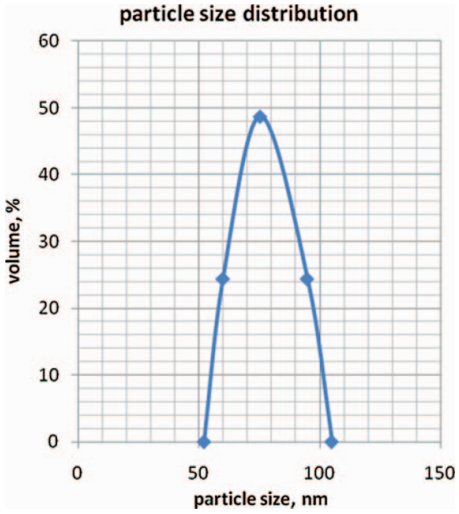

Fig. 2. The size distribution of chitosan nanoparticles by DLS. (Color figure available online.)

hydrous radii (Fig. 2). All DLS experiments were carried out at a temperature of 25.0°C and were repeated three times to check reproducibility. The size distribution profile of chitosan nanoparticles, as shown in Figure 2, represents a typical batch of nanoparticles having a narrow size distribution with the volume average hydrodynamic diameter of 75.3 nm. The morphology of chitosan nanoparticles is spherical, uniform and well dispersed as observed by scanning electron microscopy in Figure 3(C). The result of SEM was consistent with the DLS measurement in terms of nanoparticle size.

Changes in functional groups of chitosan after being nanoparticle were characterized using FT-IR spectroscopy (Fig. 1(C)). In the case of chitosan nanoparticles, the band observed in that of chitosan at 1595 cm^{-1} disappeared and a new and sharper band appeared at 1562 cm^{-1}. This change can be correlated with the linkage between the phosphoric and ammonium ions. Moreover, chitosan nanoparticles showed a peak at 1154 cm^{-1} for P = O stretching, which is also consistent with the studies of Xu et al. (26) and Knaul et al. (27).

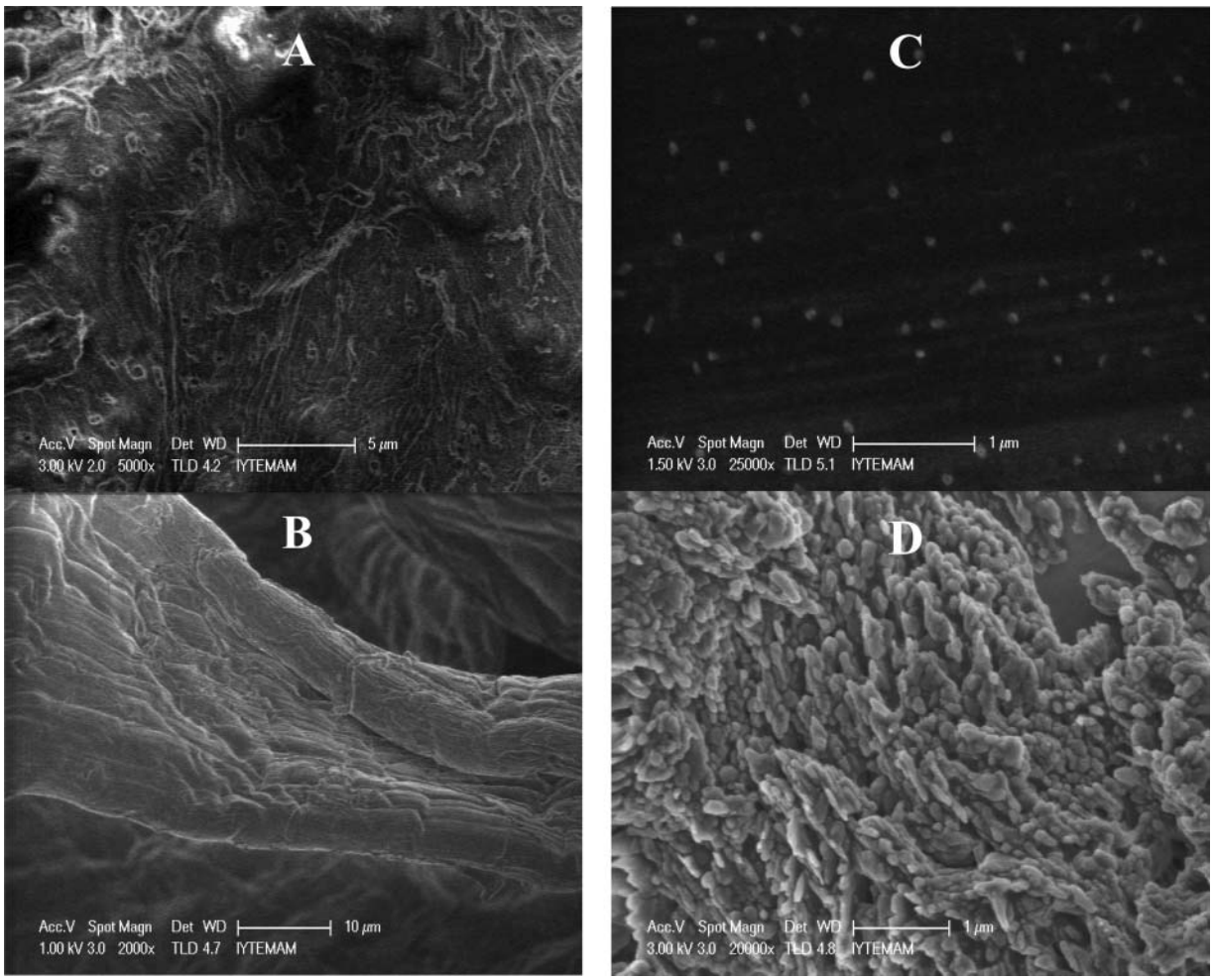

Fig. 3. Scanning Electron Microscopy Images of (A) chitin, (B) chitosan, (C) chitosan nanoparticle, (D) enzyme immobilized chitosan nanoparticles with different magnifications.

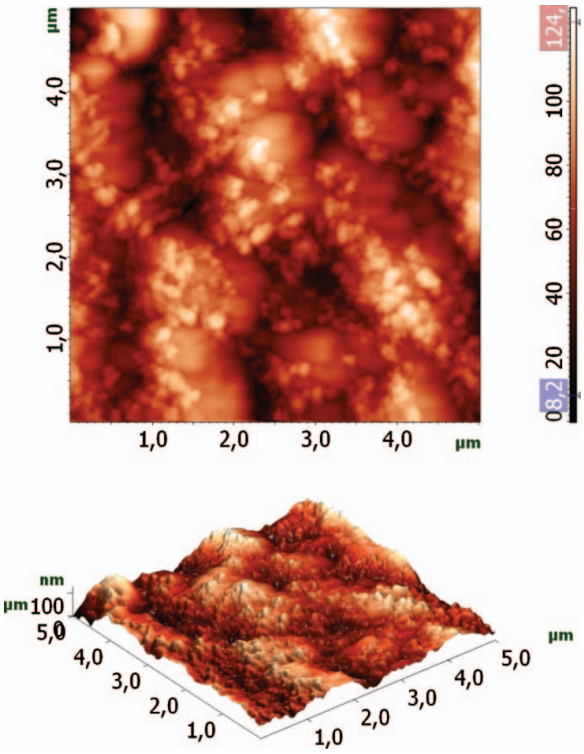

Fig. 4. AFM images of enzyme immobilized chitosan nanoparticles. (Color figure available online.)

3.3 Production, Immobilization and Characterization of Recombinant Esterase on Chitosan Nanoparticles

Production of esterase enzyme was achieved by high level expression in *E.coli* upon depression of the *lac* operator by the lactose analog IPTG. The enzyme was efficiently purified to homogeneity before immobilization procedure. As a result of heterologous expression and purification of esterase it is indicated that approximately 30.0–50.0 mg of purified active protein can be isolated with high specific activity (18). Purified thermophilic esterase enzyme was immobilized efficiently by physical adsorption onto chitosan nanoparticles. Enzyme immobilized chitosan nanoparticles were characterized by several methods. The surface morphology images by SEM reveal the increasing surface porosity of chitosan immobilized esterase in comparison to chitosan nanoparticle (Fig. 3(D)). At a higher concentration of enzyme, larger porosity was observed (data is not shown). This may indicate that the interaction between enzyme and chitosan nanoparticle is more efficient than chitosan nanoparticle with TPP. Therefore, compact and spherical shape of chitosan nanoparticle may turn to be fluffy in the presence of esterase enzyme.

Atomic force microscopy was used for visualization of the esterase immobilized chitosan nanoparticles as shown in Figure 4 and observation exhibits a regular assemblage shape. Chitosan nanoparticles are formed through the interaction of positively charged chitosan and negatively charged tripolyphosphate at room temperature. Immobilization process changes the structure and surface electric charge of chitosan due to the disruption of the secondary structure formed in its natural structure. The AFM observations are nearly same with that of SEM for the enzyme immobilized chitosan nanoparticles.

FTIR studies of enzyme immobilized chitosan nanoparticles were also performed to characterize the changes the chemical structure of chitosan nanoparticles after enzyme immobilization (Fig. 1(D)). Compared to FTIR data of chitosan nanoparticles, the peak intensity at 1650 cm^{-1} increased, two peak shifts from 1560 cm^{-1} to 1550 cm^{-1} and

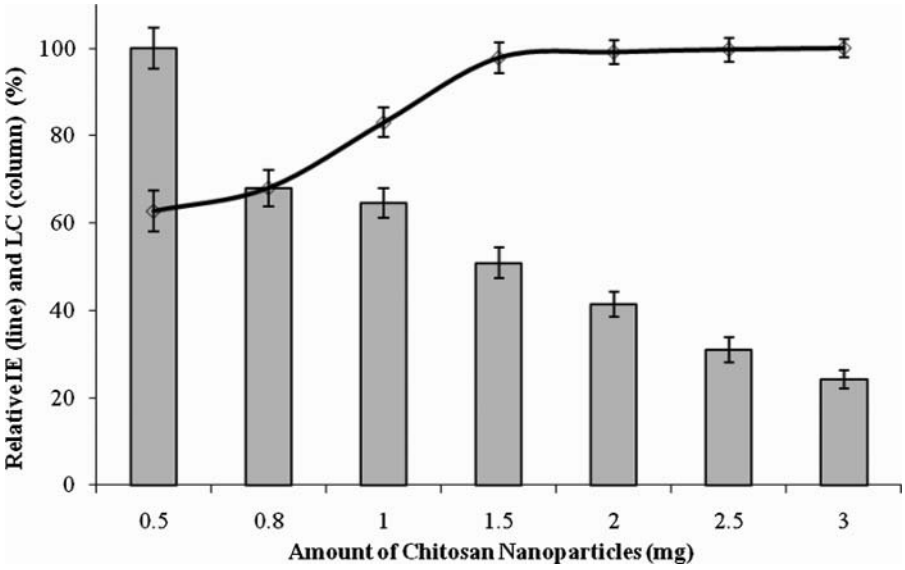

Fig. 5. The effect of chitosan nanoparticle amount on immobilization efficiency and enzyme loading capacity.

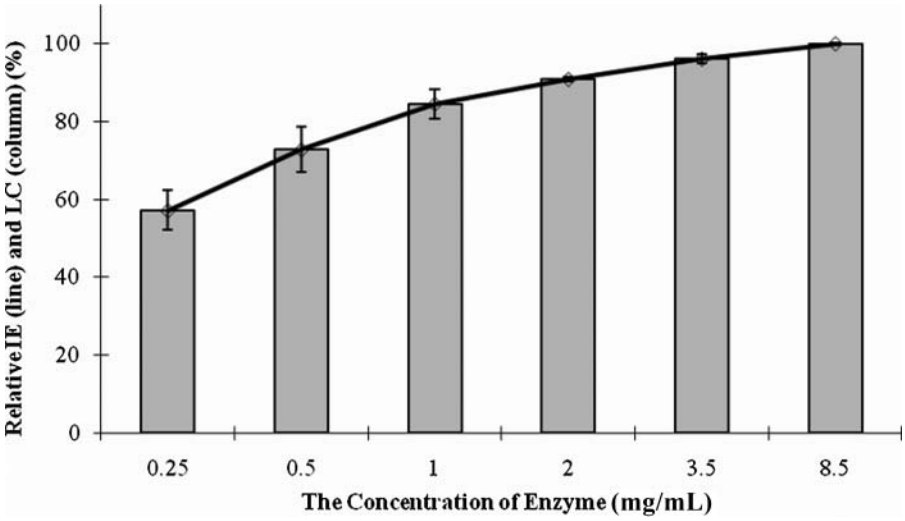

Fig. 6. The effect of enzyme concentration on immobilization efficiency and enzyme loading capacity.

from 1413 cm^{-1} to 1407 cm^{-1}were observed. The strength of these two peaks intensity were also decreased dramatically. These changes in FTIR spectrum of enzyme immobilized chitosan nanoparticles can be due to as the results of the immobilization of esterase on chitosan nanoparticles.

3.4 Optimization of Enzyme Immobilization on Chitosan Nanoparticles

For effective utilization of esterase enzyme for a variety of processes, the following immobilization parameters have been investigated in details: immobilization time, speed, pH, temperature, enzyme concentration and chitosan nanoparticle amount. In each case immobilization efficiency and enzyme loading capacity were calculated as described in Equations 1 and 2. It has been demonstrated that in a biocatalysis reaction, the enzyme efficiency and therefore cost effectiveness are greatly affected by enzyme loading on support material (28). First, the effect of amount of chitosan nanoparticles on enzyme loading capacity and immobilization efficiency of esterase were investigated (Fig. 5). The data indicates that the immobilization process is chitosan nanoparticles amount-dependent, influencing the esterase loading capacity and immobilization efficiency of the enzyme. At a constant esterase concentration, esterase immobilization efficiency has displayed a typical saturation curve with the increased amount of chitosan naoparticles (Fig. 5). The increased amount of citosan nanoparticles from 0.5 mg up to 1.5 mg shows gradual increase in immobilization efficiency of the esterase up to 88%. However, increasing amount of chitosan nanoparticles in the immobilization procedure from 1.5 mg to 3.0 mg has resulted in almost no change in terms of immobilization efficiency of

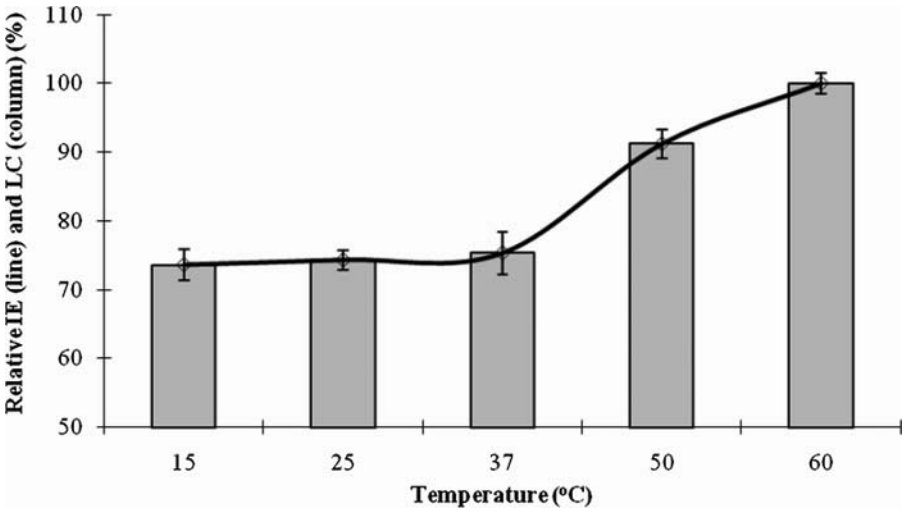

Fig. 7. The effect of temperature on immobilization efficiency and enzyme loading capacity.

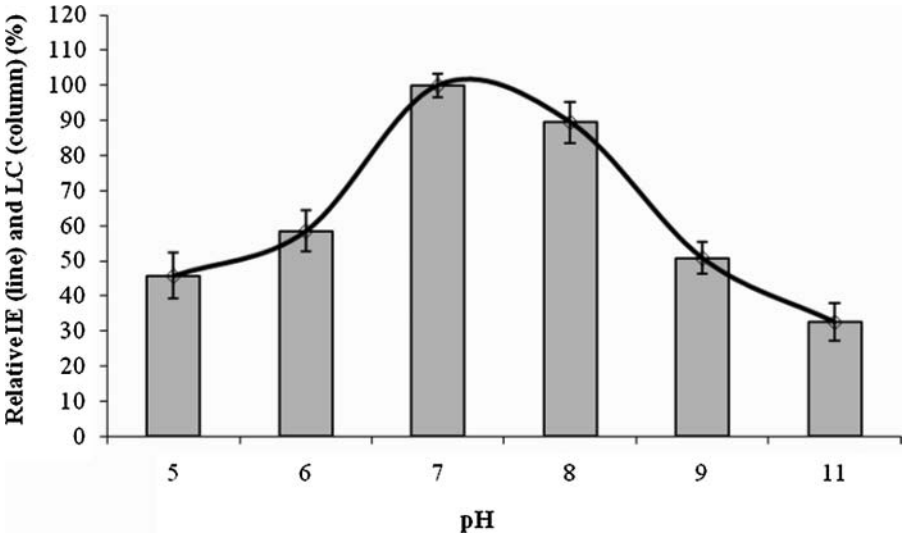

Fig. 8. The effect of pH on immobilization efficiency and enzyme loading capacity.

the esterase (from 88% to 90%). These results demonstrate that at 1.0 mg/mL esterase concentration, 1.5 mg chitosan nanoparticle amount is efficient for the optimum immobilization indicating almost all of the esterase adsorbed by the specified amount of nanoparticles. On the other hand, loading capacity of esterase on chitosan nanoparticle was decreased with the increase amount of chitosan nanoparticle at the constant enzyme concentration (Fig. 5). It can be seen that increasing the amount of chitosan nanoparticles from 0.5 mg to 3.0 mg has resulted in distribution of 1.0 mg/mL esterase throughout the nanoparticles is decreased by approximately four times. This seems likely that there is a large excess of surface area that esterase can occupy (28).

The effects of esterase concentration on immobilization procedure were evaluated and determined for the optimum immobilization condition (Fig. 6). Both relative enzyme immobilization efficiency and esterase loading capacity acted in a similar way at a constant amount of chitosan nanoparticles. Figure 6 indicates that increasing esterase concentration from 0.25 mg/mL to 1.0 mg/mL has displayed a linear increase in immobilization efficiency and esterase loading capacity, but increasing enzyme concentration from 1.0 mg/mL up to 8.5 mg/mL has resulted in a very little effect on immobilization efficiency and esterase loading capacity. Esterase (85% of 1.0 mg/mL) was immobilized on 1.0 mg/mL of chitosan nanoparticle under standard assay conditions. According to the results here, 1.0 mg/mL protein was accepted as optimal amount of protein for immobilization studies.

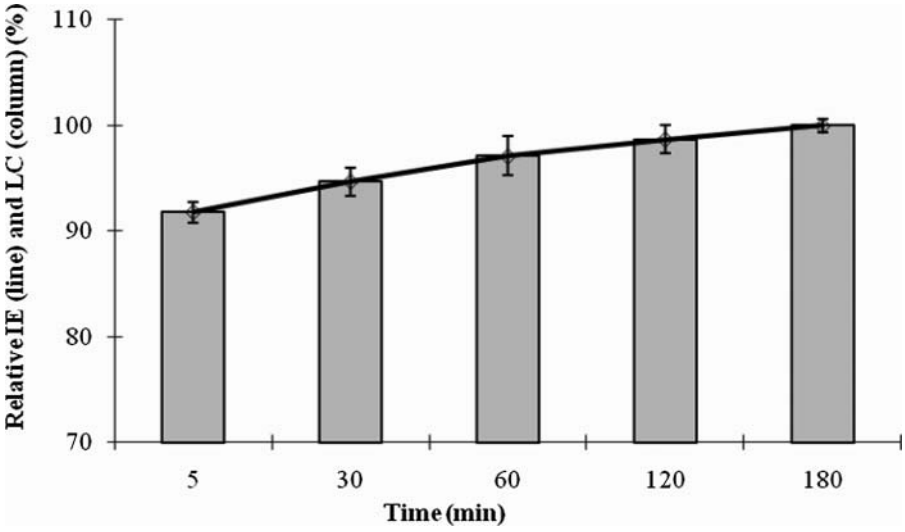

Fig. 9. The effect of immobilization time on immobilization efficiency and enzyme loading capacity.

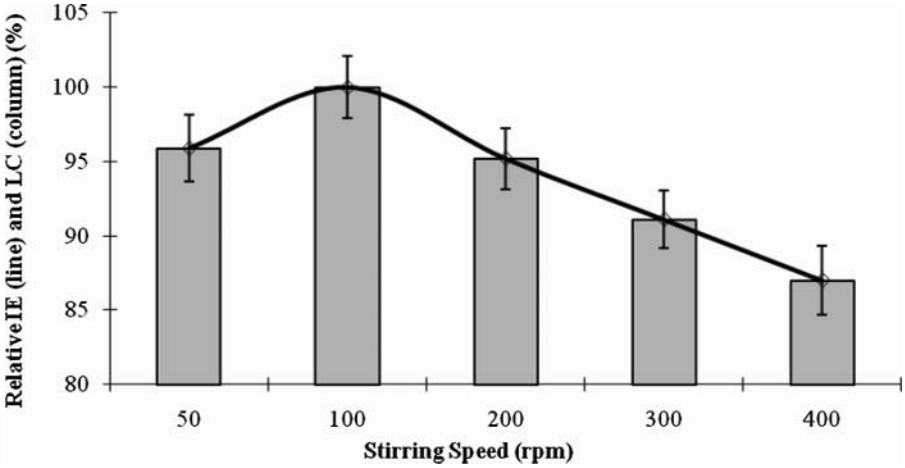

Fig. 10. The effect of immobilization speed on immobilization efficiency and enzyme loading capacity.

We believe that temperature and pH are important parameters for determination of optimum immobilization conditions. An increase in temperature up to 60°C has indicated a better immobilization efficiency and esterase loading capacity compared to low temperatures (from 10°C to 40°C) (Fig. 7). This suggests that esterase has a structure that is much easier to make as an interaction with chitosan nanoparticles at higher temperatures. This may be due to the enzyme having either a more flexible structure or a big number of potential binding sites on its surface, making it more likely to spread on the nanoparticle surface. It has also been previously demonstrated that recombinant esterase is thermophilic and shows the highest activity at 65°C (18). This finding indicates that utilization of esterase as an immobilized form with chitosan nanoparticles may elevate the optimum temperature to a higher degree. The pH dependence of the immobilization condition was investigated for esterase and chitosan nanoparticles. Relatively lower immobilization efficiency and esterase loading capacity were obtained at lower and higher pH values compared to pH 7 (Fig. 8). The adsorption process seemed to be affected due to charge interactions, and optimum immobilization was achieved at neutral pH 7. Similar pH dependence results were reported with neutral proteinase immobilization with chitosan nanoparticles (29).

The effect of immobilization time on immobilization efficiency and esterase loading capacity was tested for esterase and chitosan nanoparticles (Fig. 9). After 5 min immobilization time, 92% of immobilization efficiency and enzyme loading capacity were obtained. The immobilization procedure was very quick between esterase and chitosan nanoparticles because of their larger specific surface area of contact. Increasing immobilization time up to 3 h has resulted in a slight increase in immobilization efficiency and enzyme loading capacity. The optimal immobilization time was determined as 30 min in our studies.

Lastly, immobilization speed was investigated for the optimum immobilization condition of esterase on chitosan nanoparticles (Fig. 10). The best immobilization efficiency and enzyme loading capacity were obtained at 100 rpm. These results demonstrate that less than 100 rpm speed may not be effective for the adsorption of esterase on to nanoparticles and more than 100 rpm speed may disturb the adsorption procedure of enzyme on the nanoparticle surface.

According to our results here, the optimal immobilization conditions of esterase were determined as follows; 1.0 mg/mL esterase in 0.5 mM phosphate buffer at pH 7.0 reacted with 1.5 mg chitosan nanoparticle for 30 min at 60°C under 100 rpm stirring conditions. Under optimal conditions of the immobilization, thermophilic esterase activity yield was 88.5% compared to free esterase enzyme. The activity of recombinant esterase was slightly decreased when it was immobilized on chitosan nanoparticles. The results were not surprising because the immobilization procedure by physical adsorption may not alter the active site of thermophilic recombinant esterase.

4 Conclusions

In this study, chitosan is synthesized from chitin and chitosan nanoparticles were prepared by using the cross-linking agent TPP, and the resulting beads were employed in the immobilization process with thermophilic esterase enzyme obtained using recombinant DNA technology. The physicochemical properties of the chitosan, chitosan nanoparticles and esterase immobilized chitosan nanoparticles were determined by several methods including SEM, FT-IR, DLS and AFM. Effects of immobilization conditions on esterase immobilization efficiency and enzyme loading capacity to the nanoparticles have been examined in detail for the effective utilization of enzyme in a variety of processes.

Acknowledgements

The authors would like to thank the Center of Material Research, Department of Physics, Department of Chemical Engineering and Biotechnology & Bioengineering Research Center at İzmir Institute of Technology for the facilities SEM, AFM, DLS measurements and technical support, respectively. The authors wish to thank Dr. Mustafa Muammer Demir for his valuable contributions on SEM analysis.

References

1. Zhang, Y.F., Wu, H., and Li, J. (2008) *Chem Mater*, 20, 1041–1048.
2. Kennedy, J.F., and White, C.A. *Principles of immobilization of enzymes. In: Handbook of Enzyme Biotechnology*, Halsted Press: Chichester, New York. 1985.
3. Morales, A., Céspedes, F., and Alegret, S. (2000) *Mater. Sci. Eng. C*, 7, 99–104.
4. Coradin, T., and Livage, J. (2007) *Acc. Chem. Res.*, 40, 819–826.
5. Chen, X., Hu, Y. and Wilson, G.S. (2002) *Biosens. Bioelectron.*, 17, 1005–1013.
6. Bellezza, F., Cipiciani, A., and Costantino, U.J. (2003) *Mol. Catal. B: Enzyme*, 26, 47–56.
7. Gole, A., Dash, C., Mandale, A.B., Rao, M., and Sastry, M. (2000) *Anal. Chem.*, 72, 4301–4309.
8. Tang, Z., Qian, J., and Shi, L. (2007) *Materials Letters*, 61, 37–40.
9. Juang, R.S., Wu, F.C., and Tseng, R.L. (2001) *Bioresour. Technol.*, 80, 187–193.
10. Lee, M.K., Chun, S.K., Choi, W.J., Kim, J.K., Choi, S.H., Kim, A., Oungbho, A.K., Park, J.S., Ahn, W.S., and Kim, C.K. (2005) *Biomaterials*, 26, 2147–2156.
11. Shu, X.Z., and Zhu, K. (2002) *J. Int. J. Pharm.*, 233, 217–225.
12. Krajewska, B. (2004) *Enzyme and Microbial Technology*, 35, 126–139.
13. Berthold, A., Cremer, K., and Kreuter, J. (1996) *J. Control Release*, 39, 17–25.
14. Tian, X.X., and Groves, M.J. (1999) *J. Pharm. Pharmacol.*, 51, 151–157.
15. Faber K. (1997) *Pure Appl. Chem.*, 69, 1613–1633.
16. Quax, W.J., and Broekhuizen, C.P. (1994) *Appl. Microbiol. Biotechnol.*, 41, 425–431.
17. Panda, T., and Gowrishankar, B.S. (2005) *App. Microbiol. Biotechnol.*, 67, 160–169.
18. Tekedar, H.C., and Şanlı-Mohamed, G. (2010) *Extremophiles*, DOI 10.1007/s00792-010-0344-1.
19. Boyacı, E., Eroglu, A.E., and Shahwana, T. (2010) *Talanta*, 80, 1452–1460.
20. Tolaimate, A., Desbrieres, J., Rhazi, M., Alagui, A., Vincendon, M., and Vottero, P. (2000) *Polymer*, 41, 2463–2469.
21. Jiayin, Z., and Jianmin, W. (2006) *Chin. J. Anal. Chem.*, 34, 1555–1559.
22. Bradford, M. M. (1976) *Anal. Biochem.*, 72, 248–254.
23. Kasaai, M.R., Arul, J., and Charlet, G.J. (2000) *Polym. Sci. Part B Polym. Phys.*, 38, 2591–2598.
24. Brugnerotto, J., Lizardi, J., Goycoolea, F.M., Argüelles-Monal, W., Desbrières, J., and Rinaudo, M. (2001) *Polymer*, 42, 3569–3580.
25. Parize, A.L., Heller, M., Fávere, V.T., Laranjeira, M.C.M., Brighente, I.M.C., Micke, G.A., and Souza, T.C.R. (2009) *Latin American Journal of Pharmacy*, 28, 19–26.
26. Xu, Y., and Du, Y. (2003) *Int. J. Pharm.*, 250, 215–226.
27. Knaul, J.Z., Hudson, S.M. and Creber, K.A.M. (1999) *J. Appl. Polym. Sci.*, 72, 1721–1731.
28. Bosley, J.A., and Peilow, A.D. (1997) *JAOCS*, 74, 107–111.
29. Tang, Z.X., Qian, J.Q., and Shi, L.E. (2007) *Applied Biochem. and Biotech.*, 136, 77–96.